2023 ESMO-TAT Congress
Abstract 56P

Inhibition of HIF-2α-dependent Transcription with Small Molecule Inhibitors May Provide Therapeutic Benefit Beyond Renal Cell Carcinoma

Kelsey E. Sivick Gauthier[1,4], Soonweng Cho[1], Sadeesh K. Ramakrishnan[2,3], Dana Piovesan[1], Kenneth V. Lawson[1], Kai H. Liao[1], Paul G. Foster[1], Tzuling Cheng[1], Yatrik M. Shah[2], Matthew Walters[1]

[1]Arcus Biosciences, Hayward, CA, USA, [2]Department of Molecular & Integrative Physiology, University of Michigan Medical School, Ann Arbor, MI, USA, [3]Department of Medicine, University of Pittsburgh, Pittsburgh, PA, USA, [4]KEG is a paid employee of and owns stock in Arcus Biosciences

BACKGROUND & RESULTS

HIF-2α Biology & Research Goal

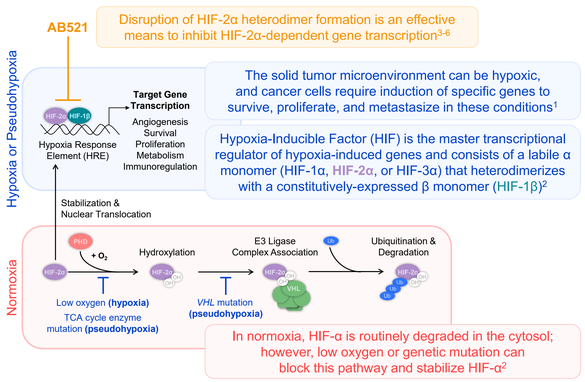

Preclinical[3,4] and clinical[7,8] evidence shows that inhibiting HIF-2α is a valid approach to block progression in pseudohypoxic cancers where HIF-2α is a tumorigenic driver.

Here, we provide additional characterization of AB521 and explore the possible clinical benefit of HIF-2α inhibition in cancers lacking pseudohypoxic mutations, namely hepatocellular carcinoma (HCC).

Characterization of AB521, a Potent Small Molecule HIF-2α Inhibitor

	SAR Assay	AB521 (mean ± SD)	belzutifan (mean ± SD)
Cell-based assays	786-O HRE Luc Reporter IC_{50} (nM)	8.2 ± 2.5	16.9 ± 10.1
	786-O HRE Luc Reporter IC_{50} [100% Serum] (nM)	46.5 ± 14.2	61.8 ± 6.6
	786-O Control Luc Reporter IC_{50} (nM)	>10,000	>10,000
	786-O VEGF-A Secretion IC_{50} (nM)	28.9 ± 3.6	47.7 ± 30.8
	Hep3B *EPO* (HIF-2α-specific) Transcript IC_{50} (nM)	35.9 ± 5.0	39.0 ± 9.7
	Hep3B *PDK1* (HIF-1α-specific) Transcript IC_{50} (nM)	>10,000	>10,000
Binding assays	Thermal Shift Assay ΔT_M (°C)	14.7 ± 0.6	12.1 ± 0.3
	MicroScale Thermophoresis K_D (nM)	2.4 ± 0.8	15.4 ± 2.7
	Isothermal Titration K_D (nM)	53.6 ± 17.9	58.3 ± 19.3
	Scintillation Proximity Assay IC_{50} (nM)	16.6 ± 5.0	22.3 ± 5.6

Table 1. Comparison of AB521 and belzutifan in cell-based and binding assays[9]. Cellular assays: Hypoxia-response element luciferase (HRE Luc) reporter and VEGF-A secretion in 786-O ccRCC cells; *EPO* or *PDK1* transcription in Hep3B HCC cells. Binding assays performed with the HIF-2α PAS-B domain. Belzutifan (MK-6482/PT2977) synthesized by Arcus Biosciences using published methodology[4]. IC_{50}, half-maximal inhibitory concentration; nM, nanomolar; SD, Standard Deviation; ΔT_M, change in melting point; °C, degrees Celsius; K_D, equilibrium dissociation constant.

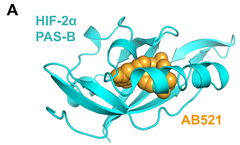

Preclinical assessment of safety and drug-drug interaction potential[9,10]:

- Low intrinsic clearance in hepatocytes
- Moderate-to-low clearance in rat and dog
- Negligible inhibition against a panel of CYP isoforms and no time-dependent CYP inhibition
- hERG IC_{50} > 10 μM

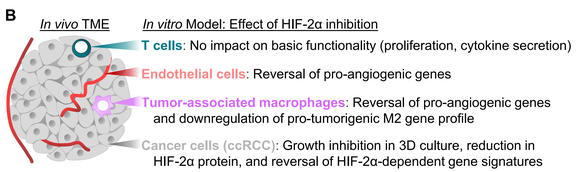

Figure 1. Structural and functional characterization of AB521. (A) X-ray co-crystal structure of HIF-2α PAS-B domain (cyan ribbon representation) shows AB521 (orange space-filling representation) binding to a small hydrophobic internal cavity of the protein. Resolution = 1.56 angstrom; R/R_{free} (%) = 17.9/20.2. **(B)** The activity of AB521 and/or predecessor/tool HIF-2α inhibitors has been evaluated upon several human cell types and described in detail elsewhere[9,11,12]. Cells present in the tumor microenvironment (TME) were modeled *in vitro* using the following: T cells = primary human peripheral CD8⁺ T cells, endothelial cells = primary human umbilical vein endothelial cells (HUVECs), tumor-associated macrophages (TAMs) = primary human CD14⁺ monocytes differentiated (M-CSF) and polarized (IL-4) to M2-like macrophages, cancer cells = 786-O ccRCC.

RESULTS

AB521 Inhibited Tumor Growth and HIF-2α Activity in Mice

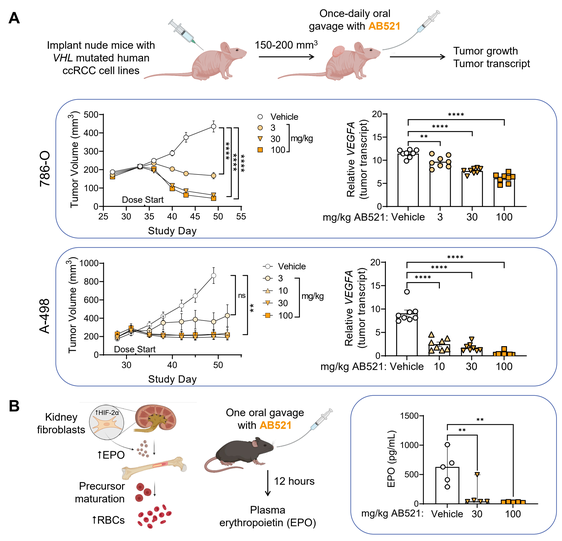

Figure 2. Efficacy and pharmacology of AB521 in mice. (A) Experimental schema. AB521 significantly inhibited progression of human 786-O and A498 ccRCC tumors and decreased tumor *VEGFA* transcript (24 hours after one dose) in a dose-dependent manner. **(B)** Overview of steady state erythropoietin (EPO) biology and experimental schema. AB521 significantly reduced plasma EPO 12 hours after one dose of AB521. ns, not significant, ****p<0.0001, **p<0.01. Growth curves: symbols and error denote mean ± SD. Bar graphs: Bars and error denote mean ± SD while symbols represent individuals. RBCs, red blood cells.

Pharmacokinetic (PK) and Pharmacodynamic (PD) Parameters Associated with AB521 in Human Healthy Volunteers

- Mean apparent terminal half-life is 18 to 24 hours, supporting once-daily (QD) dosing
- The peak-to-trough ratio is low (~2), which can help minimize potential C_{max}-related toxicity while providing sustained PD effect
- Dose-dependent reductions in serum EPO were observed following a single dose at 10 to 100 mg, with mean maximum reduction from baseline up to 85%
- Following multiple dosing (QD for 7 days), sustained EPO reduction was observed throughout the dosing period, EPO levels recovered rapidly after the end of AB521 dosing

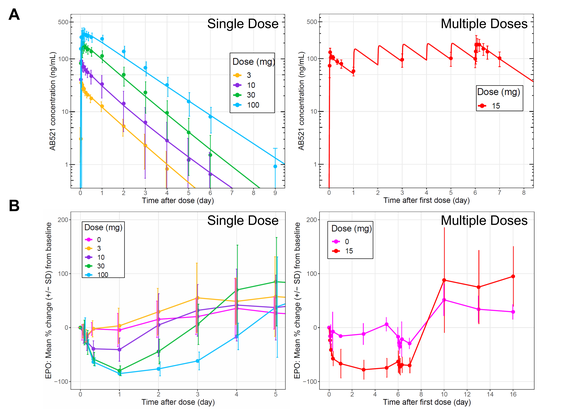

Figure 3. Pharmacokinetic (PK) and pharmacodynamic (PD) profiles of AB521 in human healthy volunteers[13] (NCT05117554/ARC-14). (A) Observed (mean ± SD) vs model-predicted (based on a preliminary population PK model) AB521 concentration-time profiles after a single or multiple oral dose(s) of AB521. **(B)** Mean ± SD serum EPO reduction-time profiles after a single or multiple oral dose(s) of AB521 or placebo. QD, once-daily.

RESULTS

Generation of Universal and Cell Line-Specific Hypoxia Gene Signatures Unique to Each HIF-α Isoform

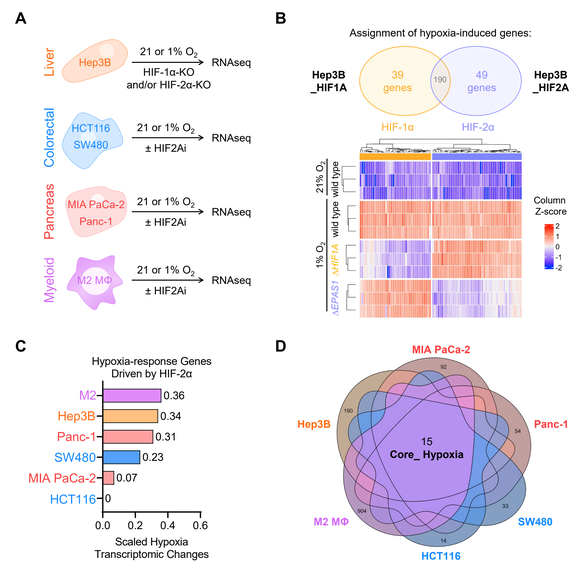

Figure 4. Derivation of Arcus hypoxia signatures. (A) Experimental schema. Various cell types were subjected to normoxic (21%) or hypoxic (1%) O_2 conditions for 24 hours prior to processing for RNA-seq. In hypoxia, cells were either treated with vehicle or 10 μM tool HIF-2α inhibitor (HIF2Ai) PT2385. In a separate experiment, pools of Hep3B cells with HIF-1α (Δ*HIF1A*), HIF-2α (Δ*EPAS1*), or both isoforms deleted were also subjected to normoxic or hypoxic conditionals prior to RNA-seq. **(B)** Shown is a Venn diagram depicting assignment of hypoxia-induced HIF isoform-specific genes in the Hep3B dataset and their expression values in the Hep3B cell lines under normoxia, hypoxia, and hypoxia with genetic knockouts of *HIF1A* or *EPAS1*. Hep3B_HIF1A (39 gene) and Hep3B_HIF2A (49 gene) signatures applied in **Figure 5** were assigned by interrogating changes in HIF-1α and HIF-2α deleted backgrounds. Dotted line demarcates unsupervised clustering. **(C)** Hypoxia-dependent transcriptomic changes for each dataset were scaled (0-1). Shown is the relative contribution of HIF-2α to the global hypoxia response for each cell type. **(D)** Shown is a Venn diagram of five cancer cell lines and M2 macrophages (MΦ) depicting the number of unique and common hypoxia-induced genes. A total of 15 genes are concordantly upregulated across all cell types and are referred to as Core_Hypoxia signature used in **Figure 5**. PT2385 synthesized by Arcus Biosciences using published methodology[14].

Hypoxia Scores are Increased with Progression of Non-alcoholic Hepatosteatosis (NASH) and Reduced with Intervention

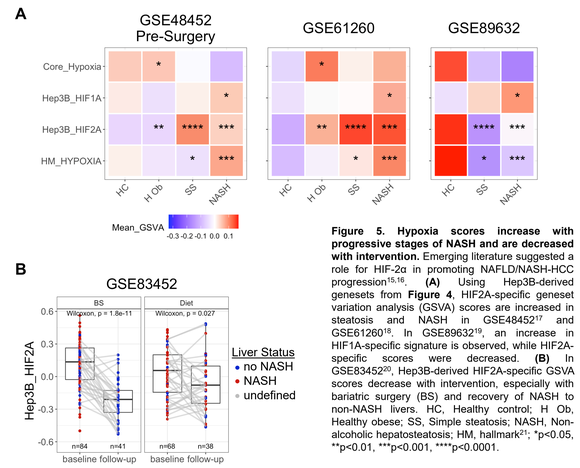

Figure 5. Hypoxia scores increase with progressive stages of NASH and are decreased with intervention. Emerging literature suggested a role for HIF-2α in promoting NAFLD/NASH-HCC progression[15,16]. **(A)** Using Hep3B-derived genesets from **Figure 4**, HIF2A-specific geneset variation analysis (GSVA) scores are increased in steatosis and NASH in GSE48452[17] and GSE61260[18]. In GSE89632[19], an increase in HIF1A-specific signature is observed, while HIF2A-specific scores were decreased. **(B)** In GSE83452[20], Hep3B-derived HIF2A-specific GSVA scores decrease with intervention, especially with bariatric surgery (BS) and recovery of NASH to non-NASH livers. HC, Healthy control; H Ob, Healthy obese; SS, Simple steatosis; NASH, Non-alcoholic hepatosteatosis; HM, hallmark[21]; *p<0.05, **p<0.01, ***p<0.001, ****p<0.0001.

RESULTS & SUMMARY

Genetic Ablation or Pharmacological Inhibition of HIF-2α Controls Tumor Progression in a NASH-Driven HCC Model

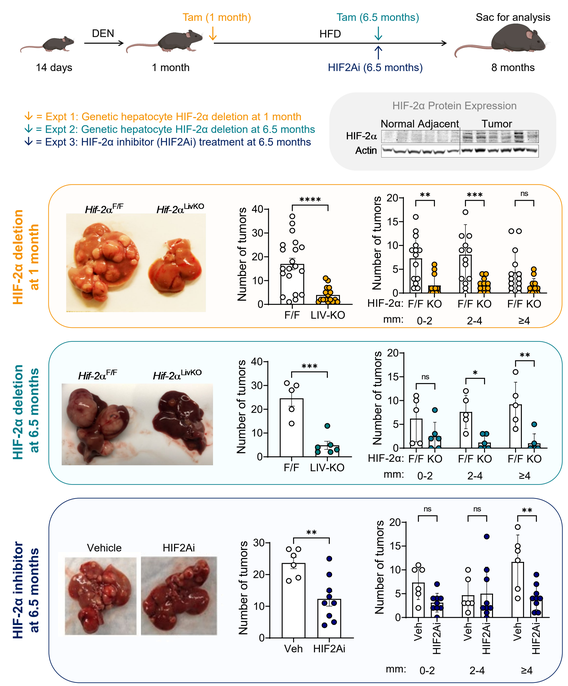

Figure 6. HIF-2α activity in hepatocytes is necessary for optimal tumor progression in a mouse model of NASH-driven HCC. Experimental schema: The role of HIF-2α in HCC tumor progression was analyzed in the diethylnitrosamine (DEN)-high-fat diet (HFD) HCC mouse model[22] using three distinct experimental setups. Mice were injected intraperitoneally (IP) with 25 mg/kg DEN at 2 weeks of age and put on a 60% HFD *ad labium* at 4 weeks of age to initiate tumor formation. Hif-2α$^{F/F}$ x Albumin-CreER^{T2} mice (LIV-KO or KO) or littermate controls lacking Cre (F/F) were used to temporally delete HIF-2α selectively in hepatocytes using tamoxifen (Tam) administration (200 mg/kg IPx2 loading followed by monthly IP) early (Expt 1: maize) or late (Expt 2: teal) in tumor development. Wild type C57BL/6 mice were used in the therapeutic HIF-2α inhibitor study (HIF2Ai, 25 mg/kg PT2385 oral gavage every other day; Expt 3: blue). Expt, experiment; Veh, vehicle; mm, millimeters.

Summary

- AB521 is a potent and selective small molecule HIF-2α inhibitor that has been thoroughly characterized in biophysical, biochemical, and cell-based assays (**Table 1** & **Figure 1**)[9-12]
- When administered orally in mice, AB521 regressed established 786-O and A498 ccRCC xenograft tumors and decreased PD markers associated with HIF-2α in the tumor and periphery (**Figure 2**)
- AB521 demonstrated PK/PD properties in healthy human volunteers that are consistent with a potential best-in-class HIF-2α inhibitor profile (**Figure 3**)[13]
  - Based on the potency-corrected exposure of the approved belzutifan dose, we anticipate the ability to explore higher doses of AB521 clinically
- Arcus-derived hypoxic gene signature score assessments in publicly available transcriptional datasets suggest utility for AB521 beyond ccRCC, particularly in NAFLD/NASH-driven HCC (**Figure 4** & **Figure 5**)
- HIF-2α promotes tumor progression in a chemically-induced NAFLD-driven mouse model of HCC, and therapeutic treatment with a HIF-2α inhibitor resulted in significant reduction in tumor burden (**Figure 6**)
- Phase 1 clinical evaluation of AB521 in subjects with ccRCC and other solid tumors has been initiated using a pharmacologically active dose of AB521 and is ongoing (NCT05536141)

References

1) Hockel (2001).J Natl Cancer Inst 10.1093/jnci/93.4.266
2) Trriner (2016).JCI 10.1172/JCI84430
3) Wallace (2016) Nature 10.1158/0008-5472.CAN-16-0473
4) Xu (2019).J Med Chem 10.1021/acs.jmedchem.9b00719
5) Li (2019).J Med Chem 10.1021/acs.jmedchem.8b01596
6) Yu (2019).Drug Disc Today 10.1016/j.drudis.2019.09.008
7) Jonasch (2022) JCO 10.1200/JCO.2022.40.16_suppl.4509
8) Jonasch (2022) JCO 10.1200/jco.2022.40.16_suppl.4546
9) Gauthier (2021) Mol Cancer Ther 10.1158/1535-7163.TARG-21-P206*
10) Lawson (2021) Cancer Res 10.1158/1538-7445.AM2021-1206*
11) Gauthier (2019) Mol Cancer Ther 10.1158/1535-7163.TARG-19-C050/
12) Gauthier (2020).JITC 10.1136/jitc-2020-SITC2020.0583
13) Liao (2022) Eur J Cancer 10.1016/S0959-8049(22)00856-5*
14) When (2018).J Med Chem 10.1021/acs.jmedchem.8b01196
15) Chen (2019) Aging 10.18632/aging.102488
16) Foglia (2021) Cell Mol Gastroenterol Hepatol 10.1016/j.jcmgh.2021.10.002
17) Ahrens (2013) Cell Metab 10.1016/j.cmet.2013.07.004 (GSE48452)
18) Horvath (2014) PNAS 10.1073/pnas.1412759111 (GSE61260)
19) Arendt (2015) Hepatol 10.1002/hep.27695 (GSE89632)
20) Lefebvre (2017) JCI Insight 10.1172/jci.insight.92264 (GSE83452)
21) Liberzon (2015) Cell Syst 10.1016/j.cels.2015.12.004
22) Márquez-Quiroga (2022) Biochem Pharmacol 10.1016/j.bcp.2021.114845

Contact: kgauthier@arcusbio.com; mwalters@arcusbio.com

*Available for download at https://arcusbio.com/our-science/publications/